Engineering Solid Mechanics 10 (2022) 287-298

Contents lists available at GrowingScience

Engineering Solid Mechanics

homepage: www.GrowingScience.com/esm

Numerical model of interation of package of open shells with a weakly compressible filler in a friction shock absorber

A. Velychkovych[a*]

[a]*Ivano-Frankivsk National Technical University of Oil and Gas, Ukraine*

ARTICLE INFO

Article history:
Received 26 January 2022
Accepted 25 March 2022
Available online
25 March 2022

Keywords:
Damping
Vibration protection
Threaded joint
Self-unscrewing
Shell package
Coefficient of friction

ABSTRACT

The problems of protecting equipment, structures and operators from the harmful effects of vibrations are among the most painful topics of modern mechanical engineering. In this research an original design of a friction shock absorber is presented in which the principle of operation is based on the contact interaction of a package of open shells with weakly compressible deformable filler. The proposed design is simple and technologically advanced, suitable for operation under high dynamic loads and at the same time has a compact transverse dimension. Such shock absorbers are projected to be used in the mining and oil and gas industries. A finite element model of a friction shock absorber with two contact pairs has been constructed: the first contact pair is "filler - package of open shells"; the second contact pair is "inner shell of the package - outer shell". The contacting bodies were presented as separate arrays of finite elements and the conditions of frictional interaction on the contact surfaces were set in the form of Coulomb's law. We considered the behavior of such a structurally nonlinear system under the action of a monotonic and nonmonotonic load. In the course of the study, the main operational characteristics of the shock absorber including the strength, rigidity, hysteresis characteristics and natural frequencies were determined. The possibility of adjusting the rigidity and shock-absorbing characteristics of the proposed device is discussed.

1. Introduction

The tasks of vibration protection are usually associated with ensuring the reliability of equipment operation under conditions of vibration and shock loads, protecting buildings, facilities and structures from operating vibration and shock machines. The relevance of such problems stimulates and maintains the interest of specialists in research in the theory of vibrations of mechanical systems and in the scientific field of dynamics and strength of machines. Vibration protection methods can be globally divided into methods that affect the vibration source, the path between the source and the vibration protection object, or the vibration protection object itself. An example of vibration source control is machine balancing (Wang et al., 2020). An example of controlling a vibration protection object is the correct setting of a machine or mechanism, i.e. ensuring that the natural frequencies do not match the forced frequencies (Yatsun et al., 2020). An example of control by transferring vibration loads is the use of vibration isolators (Chen et al., 2019). Vibration processes that occur during the operation of mining, drilling and oilfield equipment can lead to undesirable consequences (Zhu et al., 2019). In most cases, vibrations impair the strength, reliability, and durability of drilling and other downhole equipment, above-ground installations and structures, and also adversely affect the health of operators and maintenance personnel (Wada et al., 2018; Feng et al., 2018; Maeda et al., 2019).

Pipe strings used in the oil and gas industry contain a large number of threaded joints. Premature failure and inadvertent

* Corresponding author.
E-mail addresses: a_velychkovych@ukr.net (A. Velychkovych)

doi: 10.5267/j.esm.2022.3.002

self-loosening of threads under vibration loading is a common problem in various industries. This phenomenon can lead to significant financial losses due to the need for regular maintenance of connections, as well as cause emergency situations (Kopei et al., 2022; Ropyak et al., 2021). To avoid these problems, it is proposed to reduce the dynamic load of threaded joints using vibration protection systems (Gong et al., 2021), as well as to apply various locking methods (Shatskyi et al., 2020). The introduction of innovative mining technologies and the use of sophisticated rock cutting tools require complex operations, often associated with the occurrence of abnormal vibration and shock loads on equipment elements (Bazaluk et al., 2021, Ropyak et al., 2020). One of the most effective ways to solve the problems of vibration isolation of drilling and oilfield equipment is to use specialized auxiliary devices (Velichkovich, 2007; 2011; Ghasemloonia et al., 2015). To date, cushion subs (Xu, et al., 2020; Velichkovich & Dalyak, 2015), dynamic dampers and elastic couplings for the drill string (Dutkiewicz et al., 2018; Velichkovich et al., 2001; Silva et al., 2021), dampers for sucker rod strings (Velychkovych et al., 2020) have a wide practical application. The main working units of such vibration isolation systems are elastic elements.

There are a number of specific requirements for elastic elements for downhole shock absorbers. First of all, this is a compact transverse dimension of the elastic element, which is significantly limited by the borehole diameter. At the same time, the performance characteristics of the elastic element should allow it to be used under high dynamic loads, temperature differences, and the presence of an abrasive medium. Mostly, researchers are trying to adapt traditional elastic elements to such operating conditions. Their disadvantages are insufficient damping properties and a low service life under difficult operating conditions.

We offer a new shock absorber design based on a package of two open thin-walled shells. By using the proposed shell shock absorber, the disadvantages of traditional vibration protection systems will be eliminated. This will open up new prospects for the use of vibration protection systems, for example, for drill pipe assemblies, sucker rods, tubing, for building structures and construction equipment. Fig. 1 shows a schematic diagram of a shell shock absorber with high damping capacity, for which the supporting link is a package of open shells. Here, the weakly compressible filler 3 is placed in a package of cylindrical shells 2, each of which has a cut along the generatrix. Initially, the shells are mounted so that their cuts are mutually offset by an angle 180º.

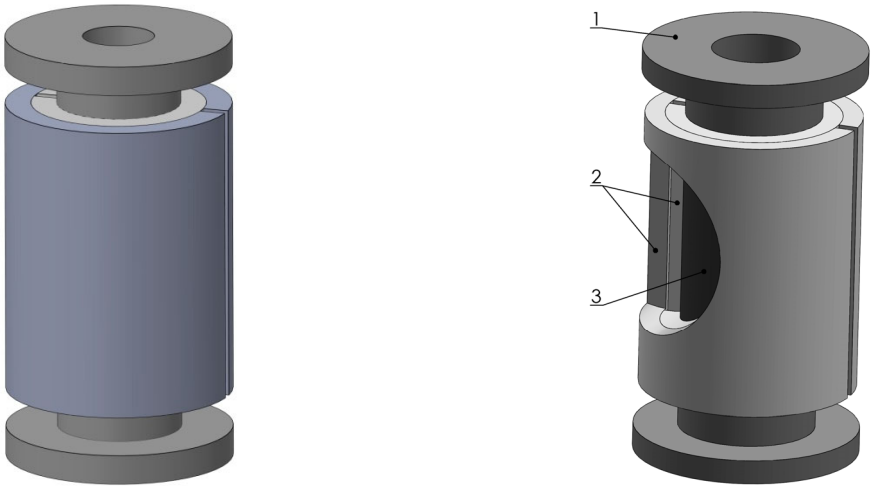

Fig. 1. Friction shock absorber, which is designed on the basis of a package of open shells:
a - general view; b - structural scheme; 1 - rigid piston; 2 - a package of two cylindrical shells, each of which has a cut along the generatrix; 3 - deformable weakly compressible filler

The deformable filler 3 is compressed by rigid pistons 1, to which an operating load is applied. As a result of contact interaction with the filler, the shell package is deformed, accumulating potential energy. Part of the energy of external influences supplied to the system is dissipated mainly due to reciprocal slipping with friction of the filler and the inner shell, as well as due to reciprocal slipping of open shells. The filler must be made of a material with a low shear modulus (so that it changes shape easily), but at the same time, this material must have a high bulk modulus (to cause the shell package to deform). Usually, we use elastomers as a filler, the rheological properties of which create an additional reserve for improving the deforming and damping properties of the shock absorber.

A correct approach for modeling and analyzing the behavior of the described shell shock absorber requires representing the structure under consideration as a layered system with two contact pairs with dry friction. The first contact pair is "deformable weakly compressible filler - package of open shells"; the second contact pair is "inner shell of the package - outer shell of the package". When considering such a system under the action of a nonmonotonic load, we obtain a constructively

nonlinear contact problem, the exact analytical solution of which is very difficult to obtain. When setting contact problems, researchers pay considerable attention to the analysis of the strength, rigidity, and stability of the contacting elements (Popov, 2010; Shatskyi et al., 2018; Bedzir et al., 1995; Ropyak et al., 2020). Analytical and numerical models of contact interaction of rod systems with the environment are considered in studies (Velychkovych et al., 2019; Shatskyi et al., 2019; Dutkiewicz et al., 2021). A class of problems on modeling the contact of cut edges or edges of crack-like defects in cylindrical shells is presented in (Shats'kyi, 2005; Shats'kyi & Makoviichuk, 2009; Shats'kyi et al., 2019).

The previous work of the authors includes approaches to studying the contact interaction of a slotted cylindrical shell with an elastic body by means of virtual and laboratory experiments and using asymptotic analytical methods (Velichkovich et al., 2018; Velychkovych et al., 2021; Shats'kyi et al., 2021). The study of the contact interaction of a weakly compressible filler with a package of open shells has never been carried out so far. The results of our study should help fill this theoretical gap. The purpose of this study is to build a finite element model of a friction shock absorber based on a package of two open shells. The model should take into account all the essential parameters of the object of study and allow the assessment of the strength, rigidity and damping characteristics of the shock absorber.

2. Materials and Methods

2.1. General Scheme of Research

We considered the problem of contact interaction of a weakly compressible deformable filler $(r,\beta,z)\in[0,R]\times[0,2\pi]\times[-l/2,l/2]$ with an elastic package of open shells $(r,\beta,z)\in[R,R+2h]\times[0,2\pi]\times[-l_0/2,l_0/2]$ by compressing the filler with smooth, absolutely rigid pistons with a force Q (Fig. 2).

The three-dimensional contact problem of the theory of elasticity was solved under such boundary conditions.

On the contact surface of the deformable filler with the package of shells, i.e. when $r=R$, $\beta\in(0,2\pi)$, $z\in[-l/2,l/2]$, the following conditions are true

$$\begin{cases}\sigma_r\le 0,\ [u_r]_1=0;\\ \sigma_r=0,\ [u_r]_1\ge 0,\end{cases}\quad\begin{cases}\vec{\tau}_r=f_1\sigma_r\dfrac{[\vec{v}]_1}{|[\vec{v}]_1|},\ [\vec{v}]_1\ne 0;\\ |\vec{\tau}_r|\le -f_1\sigma_r,\ [\vec{v}]_1=0.\end{cases}\tag{1}$$

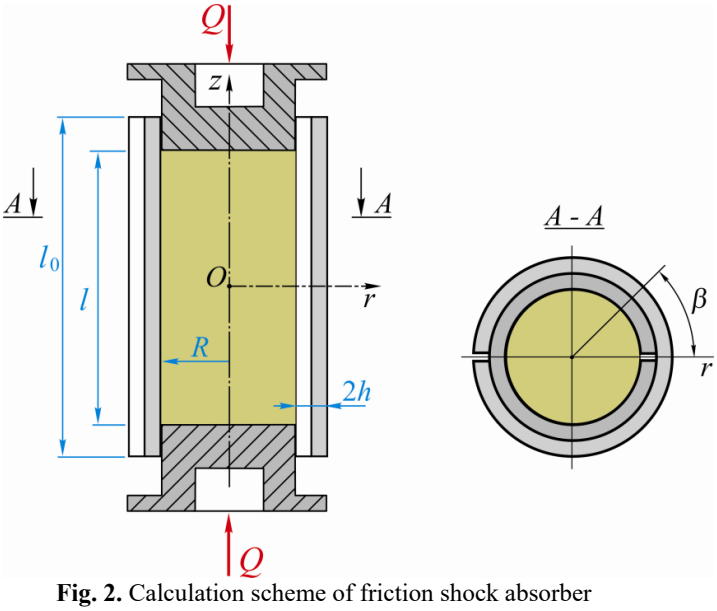

Fig. 2. Calculation scheme of friction shock absorber

At the ends of the filler at $r\in[0,R]$, $\beta\in[0,2\pi]$, $z=\pm l/2$,

$$\int_0^{2\pi}\int_0^{R}\sigma_z r\,dr\,d\beta = -Q,\ \vec{\tau}_z = 0,\ u_z = -\delta, \tag{2}$$

where Q is a set value, and δ is a required value. On the contact surface between the shells in the package, i.e. when $r = R + h$, $\beta \in [0, 2\pi]$, $z \in [-l_0/2, l_0/2]$ we will have

$$\begin{cases} \sigma_r \le 0, [u_r]_2 = 0; \\ \sigma_r = 0, [u_r]_2 \ge 0, \end{cases} \begin{cases} \vec{\tau}_r = f_2\sigma_r \dfrac{[\vec{v}]_2}{|[\vec{v}]_2|}, [\vec{v}]_2 \ne 0; \\ |\vec{\tau}_r| \le -f_2\sigma_r, [\vec{v}]_2 = 0. \end{cases} \tag{3}$$

The outer surface of the shell package is stress free, when $r = R + 2h$, $\beta \in [0, 2\pi]$, $z \in [-l_0/2, l_0/2]$

$$\sigma_r = 0, \vec{\tau}_r = 0. \tag{4}$$

Eq. (4) is also true for the part of the inner surface of the shell package located near the pistons, i.e., when $r = R$, $\beta \in [0, 2\pi]$, $|z| \in [l_0/2 - l/2, l_0/2]$.

The cut faces of each shell are free of stresses: when $r \in [R, R+h]$, $\beta = 0, 2\pi$, $z \in [-l_0/2, l_0/2]$ and when $r \in [R+h, R+2h]$, $\beta = \pi \pm 0$, $z \in [-l_0/2, l_0/2]$

$$\sigma_\beta = 0, \vec{\tau}_\beta = 0. \tag{5}$$

The ends of the package of shells are free from stresses, i.e. when $r \in [R, R+2h]$, $\beta \in [0, 2\pi]$, $z \in -l_0/2,\ l_0/2$

$$\sigma_z = 0, \vec{\tau}_z = 0. \tag{6}$$

Here $\sigma_r, \sigma_\beta, \sigma_z$ are normal stress components, and $\vec{\tau}_r, \vec{\tau}_\beta, \vec{\tau}_z$ are vectors of tangential stresses on contact surfaces, u_r, u_z are displacement components; $[\vec{v}]_1$ is a reciprocal slipping velocity vector, and $[u_r]_1$ is a displacement jump on the contact surface $r = R$; $[\vec{v}]_2$ is a reciprocal slipping velocity vector, and $[u_r]_2$ is a displacement jump on the contact surface $r = R + h$; f_1 is a coefficient of friction between filler and shell package, f_2 is a coefficient of friction between the shells in the package; l, R are the length and radius of the filler; $l_0, 2h$ is the length and thickness of the shell package.

2.2. Finite element model of friction shock absorber

The contacting bodies were filed as separate arrays of finite elements with a certain number of nodes in the contact areas. Ansys Workbench 19R2 modules were used to build the model and obtain results.

Length and radius of deformable filler $l = 0.4m$, $R = 0.08m$. The filler material is a weakly compressible rubber with a modulus of elasticity – $2 \cdot 10^7\ Pa$, shear modulus – $7 \cdot 10^6\ Pa$ and Poisson's ratio – 0.49. Given that the geometry of the filler is of high quality (there are no small details, imperfections, etc.), we used the "Hex Dominant" method to build the computational grid. As a result, we have obtained a grid based on hexahedral elements with an average element edge length of 1 cm. Formally, the shock absorber pistons are divided into final elements in a similar way. However, compared to other structural parts, pistons behave like absolutely rigid objects, so their stress-strain state has not been studied.

Length and thickness of each shell $l_0 = 0.5m$, $h = 0.01m$. The shell material is structural steel alloyed with a yield strength $\sigma_y = 700MPa$, Young's modulus – $2.1 \cdot 10^{11}\ Pa$, shear modulus – $8 \cdot 10^{10}\ Pa$ and Poisson's ratio – 0.31. The computational grid for open shells was generated using the "Tetrahedrons" method. For each shell, three-dimensional

grids were obtained with elements having the shape of a tetrahedron (with an average edge length of 1 cm). For the generation process, the Patch Independent method was used, the main idea of which is to impose a grid on the computational domain and then cut off all fragments that go beyond the geometric domain.

The frictional interaction conditions on the contact surfaces are taken in the form of Coulomb's law. Friction coefficients in contact pairs: between filler and shell package – $f_1 = 0.5$; between open shells in the package – $f_2 = 0.15$. In total, the created model of the friction shock absorber contains 73473 finite elements (Fig. 3). To obtain numerical solutions, a step-by-step process of overloading is applied with specification of the limiting conditions at each step in an iterative way. Load increments are chosen small to maintain a linear relationship between displacements and strains in each load step.

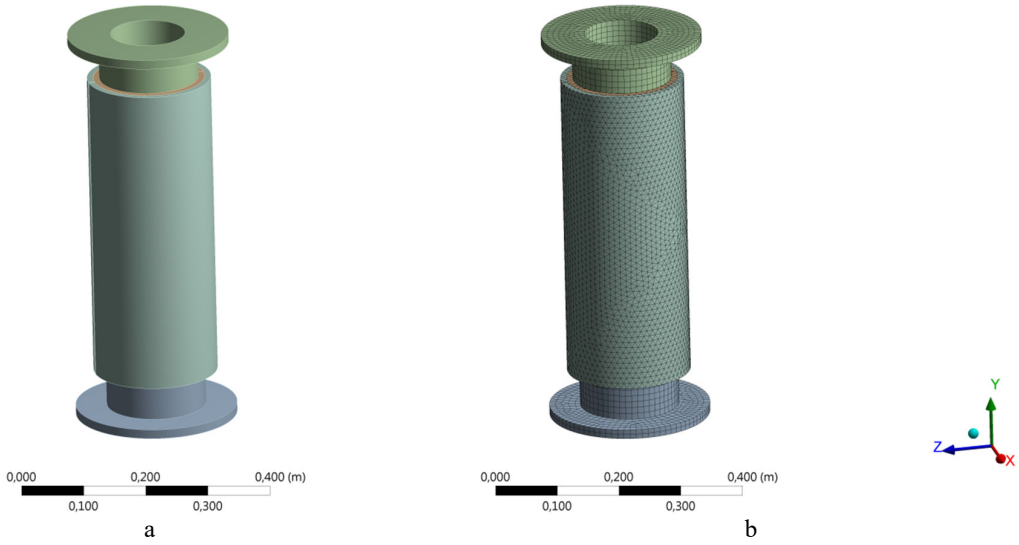

a b

Fig. 3. Finite element model of friction shock absorber:
a – geometric model; b – breakdown of the system into final elements

3. Results and Analysis

3.1 Numerical assessment of static strength of the shock absorber

The analysis of the constructed model showed that under the operational load of the shock absorber, most of the filler material and the shell package are in a complex stressed state. To determine the maximum allowable force value Q (Fig. 4a) we used the classical Mises criterion. According to this criterion, the strength of the material will be provided if the equivalent stresses (Mises stresses) σ_{eq} will not exceed the allowable stresses $[\sigma]$:

$$\sigma_{eq} = \frac{1}{\sqrt{2}}\sqrt{(\sigma_r - \sigma_\beta)^2 + (\sigma_\beta - \sigma_z)^2 + (\sigma_z - \sigma_r)^2 + 6(\tau_r^2 + \tau_\beta^2 + \tau_z^2)} \le [\sigma]. \tag{7}$$

By gradually increasing the axial force applied to the pistons, we controlled how the equivalent stresses in the material of the model changed (Fig. 4, b) and compared their values with the allowable ones. It was determined that the limiting state of the shock absorber is primarily achieved in the material of the inner shell (Fig. 4, c). Permissible stresses for the material of the open shell package:

$$[\sigma] = \frac{\sigma_y}{n} = \frac{700}{2} = 350MPa, \tag{8}$$

where n is a safety factor.

Fig. 4d shows the distributions of equivalent stresses in the most dangerous longitudinal section of the inner shell of the package. The maximum values of equivalent stresses occur in zones that are located near the planes of the ends of the filler. With the distance from the filler ends, the stresses decrease. With an external load on the shock absorber pistons $Q = 325kN$

equivalent stresses have reached the permissible value.

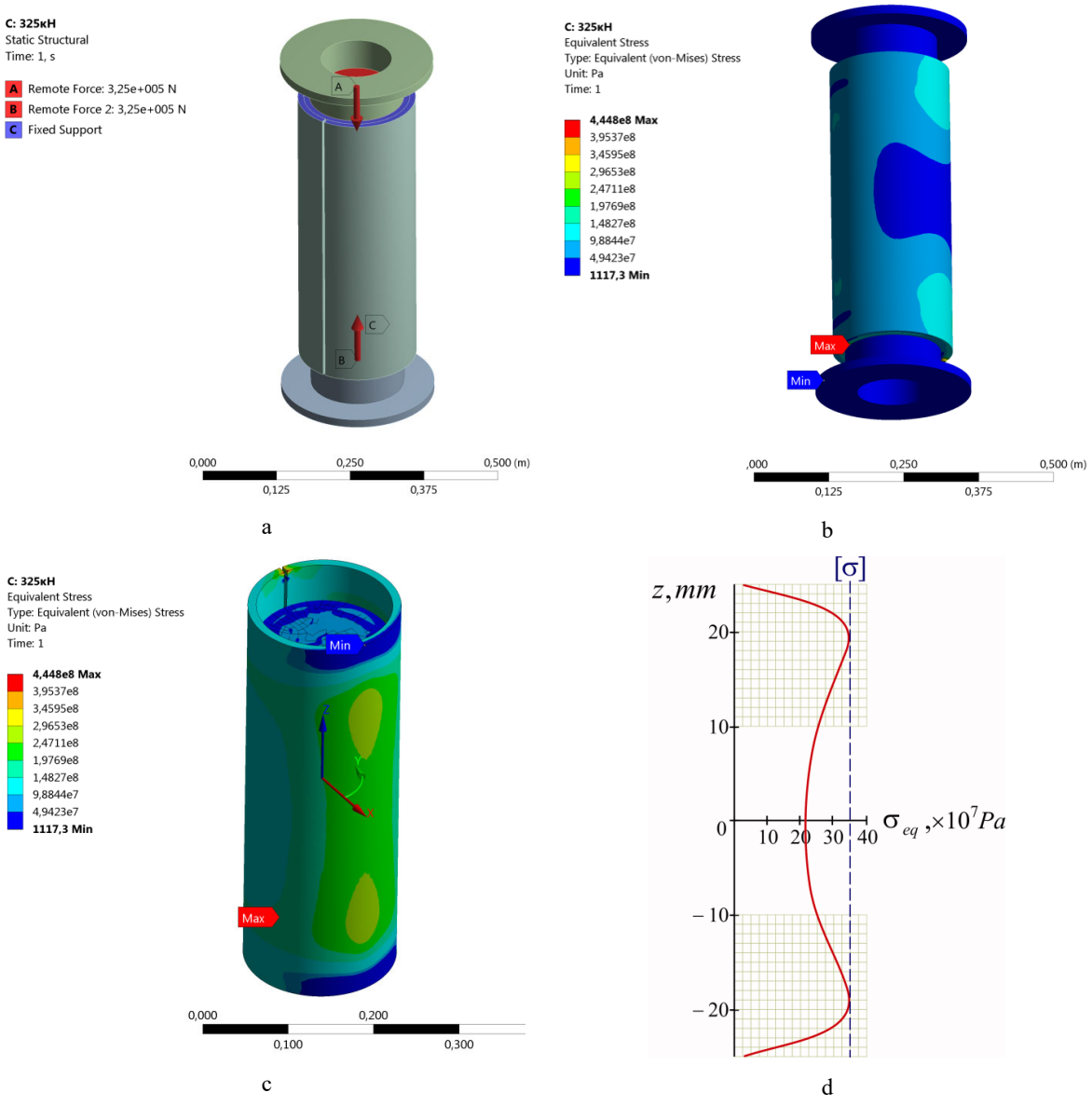

Fig. 4. Evaluation of the static strength of the friction shock absorber:
a – determination of the allowable force; b – equivalent stresses on the whole model; c – equivalent stresses on the inner shell; d – equivalent stresses in the dangerous section of the inner shell

3.2 Quasi-static diagram of shock absorber deformation

This stage of the study is devoted to the analysis of the hysteresis that occurs in the contact systems of a friction shock absorber in response to the influence of an external nonmonotonic load. Note that the mass of the shock absorber is significantly less than the mass of those structures for vibration protection of which it is used (drill string, sucker rod string, etc.). In addition, the frequencies of changes in the disturbing forces, causing the occurrence of vibrations in the systems under consideration, are less than the natural frequencies of the shock absorber. Therefore, we analyzed the hysteresis characteristics of the shock absorber using a quasi-static scheme.

When solving the task set, the typical color interpretations of the shock absorber movements, which are demonstrated by the program's postprocessor, are uninformative. For a given history of external overload, we built a shock absorber deformation diagram (Fig. 5). Here, the longitudinal deformation of the filler is plotted along the abscissa axis, that is, the ratio of the axial shock absorber draft $\delta(m)$ to the initial length of the filler $l(m)$. The ordinate shows the normal stress applied by the piston to the upper end of the filler (the integral equivalent of this stress is the axial force Q). To construct a

deformation diagram, the loading (or unloading) range was divided into a number of intervals. At each interval, the results were read, on which the diagram was built.

Let's take a closer look at the graph shown in Fig. 5. The ascending section AB depicts the stage of the initial active load from zero to 200 kN. The descending section BC characterizes the process of unloading the elastic element from the maximum external load up to 40 kN. The process of repeated active loading is depicted by the ascending segment CB. The part of the diagram depicted by lines BC - CB is the damping loop of the shock absorber. It corresponds to the force applied to the piston, which changes cyclically in time with an asymmetry factor $Q_{\min} / Q_{\max} = 40kN / 200kN = 0.2.$ With a non-monotonic shock absorber load, due to the frictional interaction of the filler with the package of shells, as well as the contact interaction between the shells in the package, part of the energy that is supplied to the system will be dissipated. The amount of energy dissipated per cycle for any load history can be calculated as the area of the damping loop of the shock absorber. In the example shown in Fig. 5, the amount of energy dissipated per cycle was 768 J.

Thus, the constructed finite element model of the shock absorber allows, based on the known history of the load, to predict its behavior at an arbitrary point in time, as well as to estimate the amount of dissipated energy.

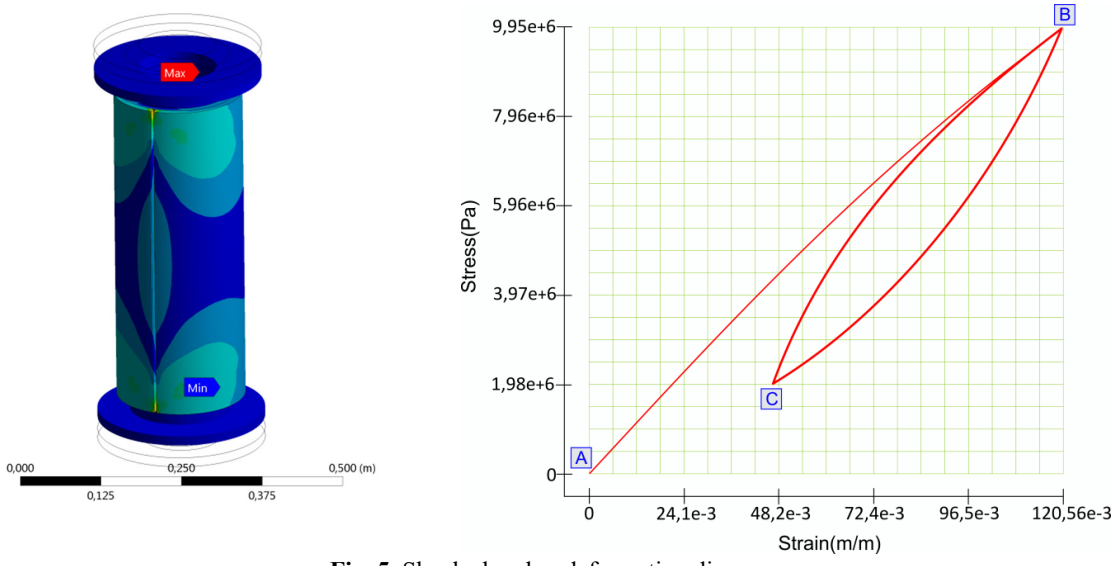

Fig. 5. Shock absorber deformation diagram:

line AB – active load from 0 to 200kN; line BC (right) – unloading from 200kN to 40kN; line CB (left) – reloading from 40kN to 200kN.

3.3. Determining the natural frequencies of the shock absorber

Typically, products undergo control tests on vibration stands, where harmonic accelerations are applied to them in a given frequency range. We implemented a similar process using the constructed finite element model of the shock absorber. To evaluate how the shock absorber design responds to a variable load acting over the expected operating frequency range, we used Harmonic Response in the ANSYS Mechanical module of the Workbench.

The model (Fig. 3b) was loaded with a cyclically variable perturbing force applied in the axial direction to the upper piston. In this case, the lower piston of the model was supported on a hard surface. The force amplitude was 1kN. The frequency of the disturbing force varied in the range of 0.200 Hz.

The first shock absorber mode is characterized by a natural frequency equal to 127.26 Hz (Fig. 6). A sufficiently large value of the natural frequency for the first mode indicates that the design is resistant to vibration action. The second mode is characterized by an even higher natural frequency equal to 154 Hz.

Interestingly, the maximum equivalent stresses for the first and second modes (Fig. 6c) occur in the same areas of the structure as under static load.

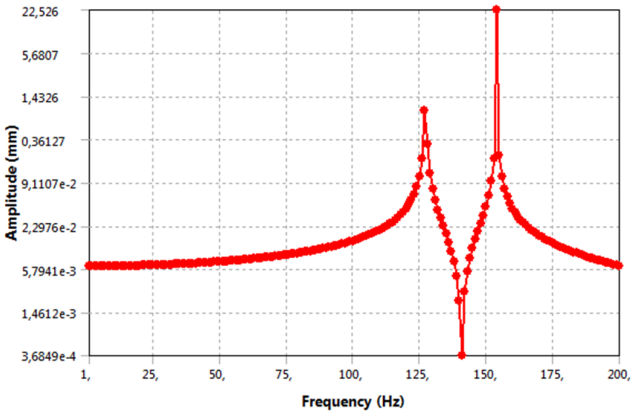

a

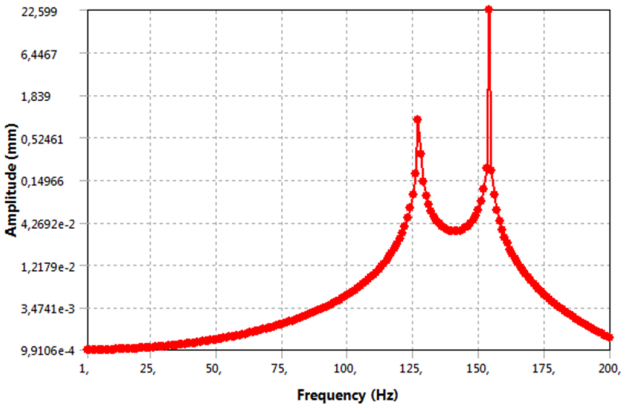

b

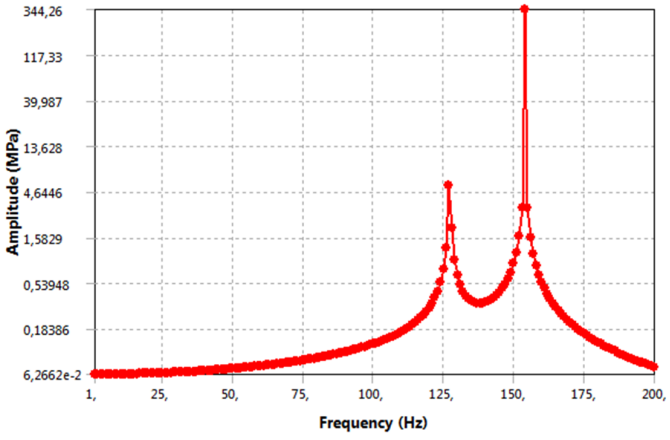

c

Fig. 6. Shock absorber natural frequencies:
a – axial displacements of the upper piston; b - axial displacements of the lower piston;
c – maximum equivalent stresses in the inner shell of the package

4. Discussion

Elastic elements with dry friction are quite often used in vibration protection systems, paying attention to the simplicity and manufacturability of structures and inexpensive maintenance. In this study, we analyze a new friction shock absorber design based on a package of two open thin-walled shells. An analysis of the behavior of the shock absorber showed that the design under consideration has good shock absorption and damping characteristics and is capable of operating under high loads with a compact transverse dimension.

Despite the results presented in the main text, let us pay attention to a number of interesting features. In the presented shock absorber, it is possible to adjust the main operational characteristic – rigidity. Rigidity adjustment is carried out by mutual displacement of shell cuts in a circular direction by a certain angle β. Fig. 7 shows three options for mounting a two-layer package of open shells of a friction shock absorber. When applying the first option, shown in Fig. 7a, we will have the minimum shock absorber rigidity. The use of the second option (Fig. 7, b) will provide the maximum rigidity of the device, and the third option (Fig. 7, c) will provide an intermediate rigidity value.

An analysis of the diagrams of normal and equivalent stresses revealed two local areas where there is a concentration of stresses. These areas can be seen in Fig. 4, c and Fig. 5, however, in order to better demonstrate them, we have chosen a characteristic cross-section of a package of open shells (Fig. 8). The first area of stress concentration is the place where the contact of the piston side surface with the cuts of the inner shell occurs. The second area is the place where the contact of the inner shell with the cuts of the outer shell occurs. When evaluating the static strength of the shock absorber, the described effects of stress concentration were not taken into account. It is planned that during the production of the shock absorber, the

described effects of stress concentration will be eliminated by technological methods (the formation of chamfers, rounding, etc.).

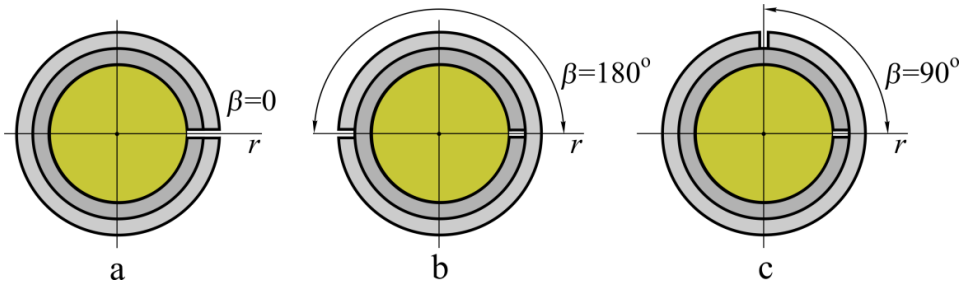

Fig. 7. The mutual location of the cuts in the package of friction shock absorber shells when adjusting the rigidity: a – minimum rigidity, b – maximum rigidity; c – intermediate rigidity value

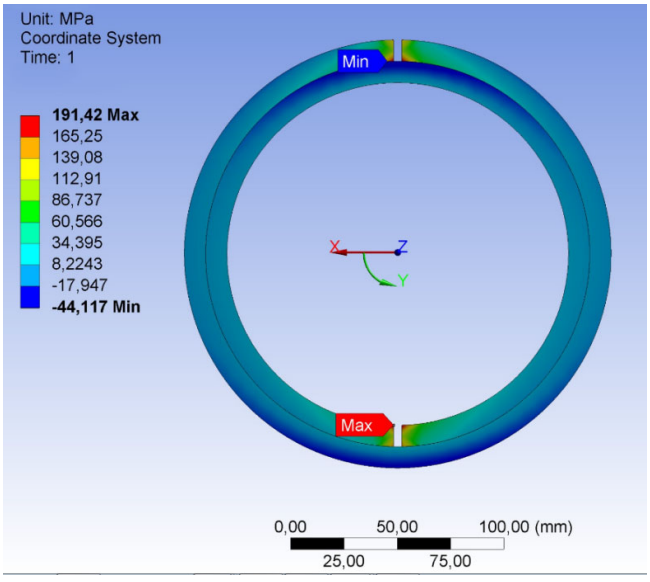

Fig. 8. Areas of stress concentration in the package of open shells.

When constructing the deformation diagram of the shock absorber, we assumed that the force applied to the piston varies cyclically over time with a coefficient of asymmetry $Q_{\min} / Q_{\max} \geq 0$. In parallel with a detailed examination of the diagram presented in Fig. 5, we observed the nature of the distribution of contact shear stresses.

It turned out that during the stage of active loading (section AB) on the entire contact surface of the pair filler - package of shells, the filler slides relative to the inner shell of the package in the direction of movement of the pistons: in the area where $z \in (0, l/2]$ slipping occurs downwards; in the area where $z \in (0, -l/2]$ slipping occurs upwards. This is evidenced by the same direction of the components of the tangential stresses τ_{rz} in the indicated contact areas. The line AB on the deformation diagram is not straight, presumably, a certain nonlinearity is caused by the fact that already at this stage there are slip and adhesion zones between the shells in the package. The descending, non-linear section of the BC characterizes the process of unloading the elastic element. At the same time, in each of the sections where the filler is in contact with the package of shells ($z \in (0, l/2]$ and $z \in (0, -l/2]$) there are two areas with different signs of the components of the tangential stresses τ_{rz}. This means that the contact area is divided into a reverse slip area and an adhesion area. During unloading, the dimensions of these zones gradually change.

If the friction shock absorber is loaded again after a slight unloading, such a reloading process will be represented by an ascending (non-linear) section of the CB. Gradually reducing the cycle asymmetry coefficient, we found such a point D (Fig. 9), from which the ascending branch of the repeated load begins to return to the section of the active load AB. For the selected shock absorber size, the value of such asymmetry coefficient is 0.1.

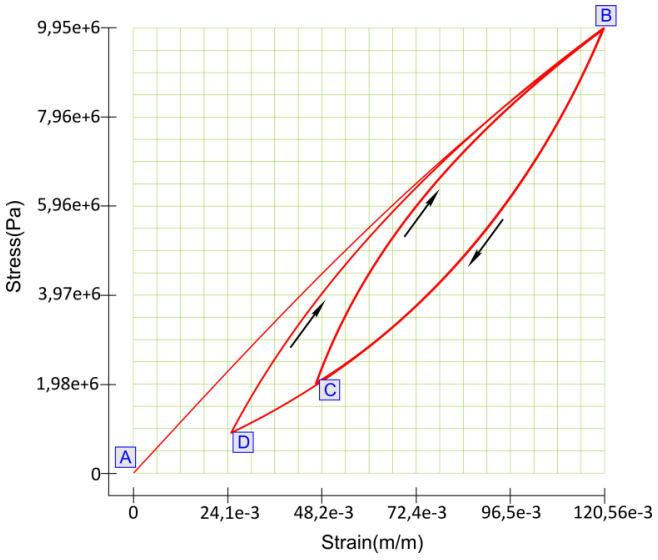

Fig. 9. Features of the deformation diagram of the friction shock absorber

With an increase in the coefficient of friction in the contact pairs ("filler - package of shells", "inner shell of the package - outer shell"), the compliance of the shock absorber decreases and the area of the damping loop decreases. At first glance, an increase in friction coefficients in contact pairs should lead to an increase in the amount of dissipated energy in one load cycle. However, it turned out that with an increase in the friction coefficient, the amount of dissipated energy decreased. This is because in systems with dry positional friction, the distribution of friction forces depends on the deformations of the contact pairs, and the deformations, in turn, depend on the friction forces. Such a close relationship determines the specific, often intuitively unpredictable features of the behavior of such structures. In this situation, an increase in the coefficient of dry friction entails a decrease in the areas of reciprocal slipping in the contact pairs of the friction shock absorber, and, consequently, a decrease in the structural energy dissipation, which occurs only in these areas.

5. Conclusions

The paper presents the original design of a friction shock absorber, in which dry friction is used to dissipate the energy of the system in order to reduce vibration loads. The main working link of the shock absorber is a two-layer package of open shells. The working body of the shock absorber is a weakly compressible deformable filler. The basic concept of a shock absorber is that it keeps moving surfaces in contact with each other, creating friction. In fact, this is a layered system with two contact pairs: the first contact pair is a "filler - package of shells"; the second contact pair is "inner shell of the package - outer shell of the package". When the system under consideration is loaded, the sizes of the slip zones in the contact areas constantly change depending on the magnitude of the load and the history of the load.

To evaluate the performance characteristics of the shock absorber, its finite element model was built. We studied the behavior of the constructed model under the action of static, quasi-static and dynamic loads. Strength assessment was carried out according to the highest equivalent stresses. Using a quasi-static non-monotonic load scheme, we built a shock absorber damping loop and determined the amount of energy dissipated in one cycle. Having done a modal analysis in the operational frequency range, we determined the natural frequencies of the shock absorber.

The analysis of the results showed that the use of a package of open shells as the main working link of the friction shock absorber made it possible to combine the high bearing capacity of the structure with a relatively low rigidity and the required level of damping. The article proposes a simple way to adjust the rigidity of the shock absorber, expanding its functionality.

References

Bazaluk, O., Slabyi, O., Vekeryk, V., Velychkovych, A., Ropyak, L., & Lozynskyi, V. (2021). A technology of hydrocarbon fluid production intensification by productive stratum drainage zone reaming. *Energies, 14*(12), 3514.

Bedzir, A. A., Shatskii, I. P., & Shopa, V. M. (1995). Nonideal contact in a composite shell structure with a deformable filler. *International applied mechanics, 31*(5).

Chen, W., Qin, Z., & Zhang, X. (2019, August). Review on the Development and Applications of Vibration Isolators. *In 2019 IEEE International Conference on Mechatronics and Automation (ICMA) (pp. 2126-2131). IEEE.*

Dutkiewicz, M., Dalyak, T., Shatskyi, I., Venhrynyuk, T., & Velychkovych, A. (2021). Stress Analysis in Damaged Pipeline with Composite Coating. *Applied Sciences, 11*(22), 10676.

Dutkiewicz, M., Gołębiowska, I., Shatskyi, I., Shopa, V., & Velychkovych, A. (2018). Some aspects of design and application of inertial dampers. *In MATEC Web of Conferences (Vol. 178, p. 06010). EDP Sciences*.

Feng, Z. M., Tan, J. J., Li, Q., & Fang, X. (2018). A review of beam pumping energy-saving technologies. *Journal of Petroleum Exploration and Production Technology, 8*(1), 299-311.

Ghasemloonia, A., Rideout, D. G., & Butt, S. D. (2015). A review of drillstring vibration modeling and suppression methods. *Journal of Petroleum Science and Engineering, 131,* 150-164.

Gong, H., Liu, J., & Ding, X. (2021). Study on local slippage accumulation between thread contact surfaces and novel anti-loosening thread designs under transversal vibration. *Tribology International, 153*, 106558.

Kopei, V., Onysko, O., Panchuk, V., Pituley, L., & Schuliar, I. (2021, September). Influence of Working Height of a Thread Profile on Quality Indicators of the Drill-String Tool-Joint. *In Grabchenko's International Conference on Advanced Manufacturing Processes (pp. 395-404). Springer, Cham.*

Maeda, S., Taylor, M. D., Anderson, L. C., & McLaughlin, J. (2019). Determination of hand-transmitted vibration risk on the human. *International Journal of Industrial Ergonomics, 70*, 28-37.

Popov, V. L. (2010). Contact Mechanics and Friction: Physical Principles and Applications, 1st ed., Springer-Verlag: Berlin, Heidelberg.

Ropyak, L. Y., Makoviichuk, M. V., Shatskyi, I. P., Pritula, I. M., Gryn, L. O., & Belyakovskyi, V. O. (2020). Stressed state of laminated interference-absorption filter under local loading. *Functional Materials, 27*(3), 638-642.

Ropyak, L. Y., Pryhorovska, T. O., & Levchuk, K. H. (2020). Analysis of materials and modern technologies for PDC drill bit manufacturing. *Progress in Physics of Metals, 21*(2), 274-301.

Ropyak, L. Y., Vytvytskyi, V. S., Velychkovych, A. S., Pryhorovska, T. O., & Shovkoplias, M. V. (2021). Study on grinding mode effect on external conical thread quality. *In IOP Conference Series: Materials Science and Engineering (Vol. 1018, No. 1, p. 012014)*. IOP Publishing.

Shats' kyi, I. P. (2005). Closure of a longitudinal crack in a shallow cylindrical shell in bending. *Materials Science, 41*(2), 186-191.

Shats'kyi, I. P., Shopa, V. M., & Velychkovych, A. S. (2021). Development of full-strength elastic element section with open shell. *Strength of Materials, 53*(2), 277-282.

Shats'kyi, I., & Makoviichuk, M. (2009). Analysis of the limiting state of cylindrical shells with cracks with regard for the contact of crack lips. *Strength of materials, 41*(5).

Shats'kyi, I. P., Makoviichuk, M. V., & Shcherbii, A. B. (2019). Influence of a flexible coating on the strength of a shallow cylindrical shell with longitudinal crack. *Journal of Mathematical Sciences, 238*(2), 165-173.

Shatskyi, I. P., Makoviichuk, M. V., & Shcherbii, A. B. (2017). Equilibrium of cracked shell with flexible coating. *Shell Structures: Theory and Applications, 4*, 165-168.

Shatskyi, I., Ropyak, L., & Velychkovych, A. (2020). Model of contact interaction in threaded joint equipped with spring-loaded collet. *Engineering Solid Mechanics, 8*(4), 301-312.

Shatskyi, I., Velychkovych, A., Vytvytskyi, I., & Seniushkovych, M. (2019). Analytical models of contact interaction of casing centralizers with well wall. *Engineering Solid Mechanics, 7*(4), 355-366.

Silva, R. S., Ritto, T. G., & Savi, M. A. (2021). Shape memory alloy couplers applied for torsional vibration attenuation of drill-string systems. *Journal of Petroleum Science and Engineering, 202*, 108546.

Velichkovich, A. S. (2007). Design features of shell springs for drilling dampers. *Chemical and Petroleum Engineering, 43*(7), 458-461.

Velichkovich, A. S., & Dalyak, T. M. (2015). Assessment of stressed state and performance characteristics of jacketed spring with a cut for drill shock absorber. *Chemical and Petroleum Engineering, 51*(3), 188-193.

Velichkovich, A. S., & Velichkovich, S. V. (2001). Vibration-impact damper for controlling the dynamic drillstring conditions. *Chemical and petroleum engineering, 37*(3), 213-215.

Velichkovich, A. S., Popadyuk, I. I., & Shopa, V. M. (2011). Experimental study of shell flexible component for drilling vibration damping devices. *Chemical and Petroleum Engineering, 46*(9), 518-524.

Velichkovich, A., Dalyak, T., & Petryk, I. (2018). Slotted shell resilient elements for drilling shock absorbers. *Oil & Gas Science and Technology–Revue d'IFP Energies nouvelles, 73,* 34.

Velychkovych, A. S., Andrusyak, A. V., Pryhorovska, T. O., & Ropyak, L. Y. (2019). Analytical model of oil pipeline overground transitions, laid in mountain areas. *Oil & Gas Science and Technology–Revue d'IFP Energies nouvelles, 74*, 65.

Velychkovych, A., Bedzir, O., & Shopa, V. (2021). Laboratory experimental study of contact interaction between cut shells and resilient bodies. *Engineering Solid Mechanics, 9*(4), 425-438.

Velychkovych, A., Petryk, I., & Ropyak, L. (2020). Analytical study of operational properties of a plate shock absorber of a sucker-rod string. *Shock and Vibration*, 2020.

Wada, R., Kaneko, T., Ozaki, M., Inoue, T., & Senga, H. (2018). Longitudinal natural vibration of ultra-long drill string during offshore drilling. *Ocean Engineering, 156*, 1-13.

Wang, Z., Zhang, B., Zhang, K., & Yue, G. (2020). Optimization and Experiment of Mass Compensation Strategy for Built-In Mechanical On-Line Dynamic Balancing System. *Applied Sciences, 10*(4), 1464.

Xu, X., Gu, H., Kan, Z., Zhang, Y., Cheng, J., & Li, Z. (2020). Properties of Drillstring Vibration Absorber for Rotary Drilling Rig. *Arabian Journal for Science and Engineering, 45*(7), 5849-5858.

Yatsun, V., Filimonikhin, G., Pirogov, V., Amosov, V., & Luzan, P. (2020). Research of Antiresonance Three-Mass Vibratory Machine With a Vibration Exciter in the Form of a Passive Auto-Balancer. *Eastern-European Journal of Enterprise Technologies, 5*(7), 107.

Zhu, Q., Zou, Z., Huang, B., Ma, L., & Xia, J. (2017). Downhole vibration causing a drill collar failure and solutions. *Natural Gas Industry B, 4*(2), 73-80.